

Voltage- and Flow-Controlled Electrodialysis Batch Operation: Flexible and Optimized Brackish Water Desalination

Wei He^{a,b,1,*}, Anne-Claire Le Henaff^{a,1}, Susan Amrose^a, Tonio Buonassisi^a, Ian Marius Peters^a, Amos G. Winter, V^a

^a*Department of Mechanical Engineering, Massachusetts Institute of Technology, Cambridge, MA, 02139, United States*

^b*School of Engineering, University of Warwick, Coventry, CV4 7AL, United Kingdom*

Abstract

Electrodialysis (ED) desalination has been demonstrated to be more energy-efficient, provide higher-recovery, and be lower-cost for producing drinking water from saline groundwater compared to reverse osmosis. These benefits of ED could translate into cost-effective, renewable-powered desalination solutions. However, the challenge of using a variable power source (e.g. solar) with traditional steady-state ED operation requires batteries to reshape the power source to match the desalination load; these batteries often contribute to a large fraction of the produced water cost. In this study, we propose a time-variant voltage- and flow-controlled ED operation that can enable highly flexible desalination from variable power sources, including renewables, with negligible batteries, potentially leading to reduced water costs compared to what existing technology can provide. A model-based controller is presented which varies applied ED stack voltage and pumping flow rate to match power consumption to a variable source while maximizing desalination rate throughout an ED batch. The utility of the controller was demonstrated with a pilot-scale system tested with brackish groundwater, which operated as expected under varying fixed power levels and a real solar irradiance profile. The pilot system achieved a production rate up to 45% higher than that of an equivalently sized traditional steady-state ED system.

Keywords:

Brackish Water Desalination, Variable Power, Electrodialysis, Variable Voltage and Flow, Model-Based Control

1. Introduction

1.1. Background

Almost two-thirds of the world's population, approximately four billion people, face severe water scarcity during at least one month of the year [1]. Pressures from population growth and climate change are expected to exacerbate this water stress by increasing water demand as water supplies become more erratic and uncertain [2]. One approach to mitigate water stress is to make use of brackish groundwater, or groundwater with a total dissolved solids (TDS) concentration above the taste threshold (>500 mg/L). Brackish groundwater is prevalent throughout the world [3, 4, 5] and is increasingly being used in the Middle East and North Africa to meet municipal water demand [6]. However, its use is limited

by the high-cost of desalination, difficulties of managing large volumes of waste brine, and the high costs of integrating with off-grid energy sources [7]. These issues are most challenging in remote, off-grid, rural communities that are prevalent in countries such as India [8], where the majority of those facing severe water scarcity live [1].

Currently, the dominant method of desalinating brackish groundwater is reverse osmosis (RO) [9]. Wright et al. demonstrated that photovoltaic (PV)-powered electrodialysis (ED) can be an energy- and cost-effective alternative solution to RO for village-scale applications, particularly suited to rural India [8]. ED has a lower energy consumption per unit water produced compared to RO (75% less at 1,000 mg/L and 30% less at 3,000 mg/L), and a greater water recovery ratio (nearly double that of current village-scale RO systems) [8]. The high energy efficiency of ED reduces its carbon footprint and translates into a smaller, less expensive renewable power systems than those required for off-grid RO, which could reduce total water costs. The high water recovery could

*Corresponding author
Email address: whe@mit.edu, Wei.He.2@warwick.ac.uk
(Wei He)

¹Shared first authorship

37 also lower water wastage and brine management costs
38 relative to RO. These combined features make ED a
39 promising technology for cost-constrained communities
40 in developing countries and water scarce regions [10].

41 Although ED is amenable to renewable power due to
42 its low specific energy consumption for brackish water
43 desalination, remaining challenges arise from balancing
44 variable renewable power sources and electrical demand
45 for producing water. A traditional static ED system typi-
46 cally operates at a constant voltage and flow rate, which
47 creates an inflexible electrical load that often requires
48 large battery banks to reshape the variable power input
49 (from a source such as solar) for meeting the desalination
50 demand throughout the day. As a result, batteries con-
51 tribute a large fraction of the lifetime cost and the total
52 water cost for an off-grid ED system [11, 12, 13]. Similar
53 challenges are also faced ED systems powered by elec-
54 trical grids with incorporated wind and solar sources;
55 to constantly meet electrical demands (including desali-
56 nation), high-cost energy storage is essential to provide
57 the flexibility that cancels out the intermittence of the
58 renewables [14, 15].

59 1.2. Benefits of time-variant desalination

60 To mitigate some of these challenges and costs asso-
61 ciated with energy storage, this study proposes a time-
62 variant ED operation by varying voltage and flow rate,
63 to catalyse the flexible use of variable power sources
64 with negligible batteries. Using the proposed flexible
65 operation, these time-variant ED systems could produce
66 more water than demanded when excess power is avail-
67 able (say on sunny time) and store it for periods when
68 power is not available (say on cloudy time); this ap-
69 proach would effectively store energy as treated water,
70 rather than storing it in batteries [13]. The flexibility
71 in utilizing variable power for water production could
72 reduce battery capacity compared to that required by
73 traditional renewable energy-powered ED systems that
74 have similar daily production rates, thereby potentially
75 reducing total water costs.

76 Flexible desalination operation also offers several ben-
77 efits to on-grid desalination. It could enable the exploita-
78 tion of variable electricity tariffs (particularly low tariffs
79 during off-peak times) to reduce energy costs for des-
80 alination, as off-peak electricity tariffs are often less
81 expensive than peak electricity tariffs [16]. Flexible
82 desalination can also aid in lowering costs and carbon
83 emissions of the electrical grid, as the flexible ED op-
84 eration could help smooth intermittent renewable power
85 and lead to less energy storage required for the supply-
86 demand balance.

87 1.3. Review of prior work

88 Several flexible operation strategies for desalination
89 have previously been explored for minimizing required
90 energy storage. Richards et al. [17] presented a flexible
91 RO brackish water desalination system under a charac-
92 terized domain of operational variables, in which the sys-
93 tem could directly utilize wind or solar power sources to
94 continuously produce water without batteries. This flex-
95 ible RO system was later experimentally demonstrated to
96 produce water under wind power at various speeds [18]
97 and solar power at several irradiance levels [19, 20].
98 Cirez et al. [21] developed a flexible PV-ED system
99 using an optimized PV module design, which was com-
100 posed of multiple connected PV cells in series/parallel
101 that could vary voltage applied to the ED stack and max-
102 imize energy transfer given available solar irradiance.
103 Malek et al. [22] demonstrated robust and stable des-
104 alination performance in a lab-scale, directly-coupled,
105 wind-powered ED system under various wind speeds,
106 turbulence intensities, and periods of oscillation. Veza
107 et al. [23, 24] actively controlled the flow rate and
108 voltage of a wind-powered ED system by developing a
109 database of correlations between available energy, prod-
110 uct concentration, flow rate, and voltage applied to the
111 two ED stacks in the system.

112 Each of these systems adjusted water production rates
113 to maximize utilization of the variable power resource.
114 However, none of these prior studies presents a deter-
115 ministic model for how to control the voltage and flow
116 rate of an ED system to utilize all available power from a
117 variable power source while maximizing water produc-
118 tion rate. In water-stressed, cost-constrained settings,
119 the utility of maximizing production is to increase the
120 number of people who can gain access to potable wa-
121 ter. Furthermore, maximizing water production from
122 a finite system size can lead to smaller, lower-cost ED
123 systems by improving the productivity per unit material
124 (e.g. membranes).

125 1.4. Objectives of this study

126 The objective of the present study is to develop and
127 demonstrate a highly-flexible, time-variant ED operation
128 strategy that can accommodate variable power sources.
129 This work is built on our previous research focused on
130 PV-ED system cost optimization with a flexible on-off
131 control strategy proposed by Bian et al.[13], which max-
132 imizes utilization of solar power on a day-by-day basis
133 to reduce required battery capacity, and a voltage con-
134 trolled strategy proposed by Shah et al. [25], which max-
135 imizes water production rate by continuously changing
136 the voltage applied to an ED stack to operate near lim-
137 iting current density throughout a batch. In the present

138 study, by introducing a new degree of freedom in control
 139 – flow rate – the proposed flexible ED operation can si-
 140 multaneously maximize drinking water production and
 141 variable power utilization. This is achieved by actively
 142 optimizing and controlling the voltage applied to an ED
 143 stack and the flow rate through it. To create, validate,
 144 and explore this highly-flexible ED technology, this pa-
 145 per we:

- 146 1. codify the flexibility of batch ED operation given
 147 voltage- and flow-controlled operation, and their
 148 impact on water production;
- 149 2. develop a model-based controller that simultane-
 150 ously co-maximizes water production rate and vari-
 151 able power utilization; and
- 152 3. validate the controller using a pilot-scale time-
 153 variant ED system and benchmark its performance
 154 relative to conventional static ED operation.

155 2. Electrodialysis desalination and time-variant op- 156 eration

157 2.1. Electrodialysis desalination

158 ED is an electrochemical process that removes ions us-
 159 ing an external electric field with selective ion-exchange
 160 membranes. In an ED system (Fig. 1), saline water
 161 flows through an ED stack which contains a series of al-
 162 ternating anion exchange membranes (AEM) and cation
 163 exchange membranes (CEM). AEMs only allow passage
 164 of anions and CEMs only pass cations. With an elec-
 165 tric field applied over the ED stack, anions flow towards
 166 the anode and cations towards the cathode. Therefore,
 167 the placement of AEMs and CEMs in series selectively
 168 controls the ion removal across the membranes, and pro-
 169 duces alternating channels of diluate and concentrate.

170 There are two types of ED operation: continuous, in
 171 which a saline feed is desalinated within a single pass
 172 through multiple ED stages (Fig. 1a); and batch, in
 173 which diluate and concentrate are recirculated through a
 174 single-stage ED stack until the diluate is desalinated to
 175 a desired product concentration (Fig. 1b). Compared to
 176 continuous ED, batch ED potentially requires a smaller
 177 stack, a smaller footprint, less membrane area, and lower
 178 capital costs to build a small-scale desalination system
 179 [13, 26, 25]. Based on these advantages, this study
 180 focuses on batch ED operation.

181 2.2. The concept and advantages of voltage- and flow- 182 controlled ED operation

183 Figure 2 illustrates the advantages of voltage- and
 184 flow-controlled ED operation, namely through improved

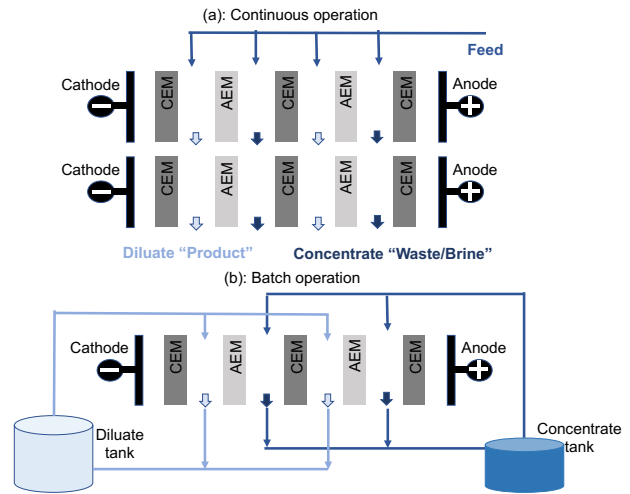


Figure 1: Schematic of ED desalination operation. In ED, an electric field is applied across alternating cation (CEM) and anion (AEM) exchange membranes to transport ions from the diluate channels to the concentrate channels. In a continuous ED system (a), feed is often passed through multiple ED stacks to produce product water. In an batch ED system (b), diluate and concentrate are recirculated through a single ED stack until the diluate is desalinated to a desired product concentration.

operational flexibility and water production compared to
 conventional static ED operation and voltage-controlled
 ED operation. The term “flexibility” in this study refers
 to the variability of power at which the ED system is
 able to operate. Figure 2a depicts a typical power con-
 sumption pattern during a static ED batch, in which a
 constant voltage and a constant flow rate are applied.
 At each diluate concentration, as the batch desalinate
 from feed to product, the power consumption is fixed
 regardless of input power available. Static ED opera-
 tion does not have any flexibility, requiring the power
 source (e.g. the grid or a solar system with batteries)
 to be able to match the fixed desalination power de-
 mand. Figure 2d depicts the current density through-
 out a batch static ED process, which represents the ion
 transfer rate across the membranes. With higher ap-
 plied current density the system can desalinate faster.
 The limiting current density determines the maximum
 salt removal rate before splitting water [25]. To avoid
 water splitting, in a conventional static ED batch, the
 applied voltage is determined by setting the current
 density below the most constraining limiting current
 density, which occurs at the end of the batch (Fig. 2d).
 As a result of this constraint, the applied current den-
 sity is much lower than limiting at other points in the
 batch process, resulting in underutilized capacity of
 the membranes throughout much of the batch, and a
 salt removal rate that is lower

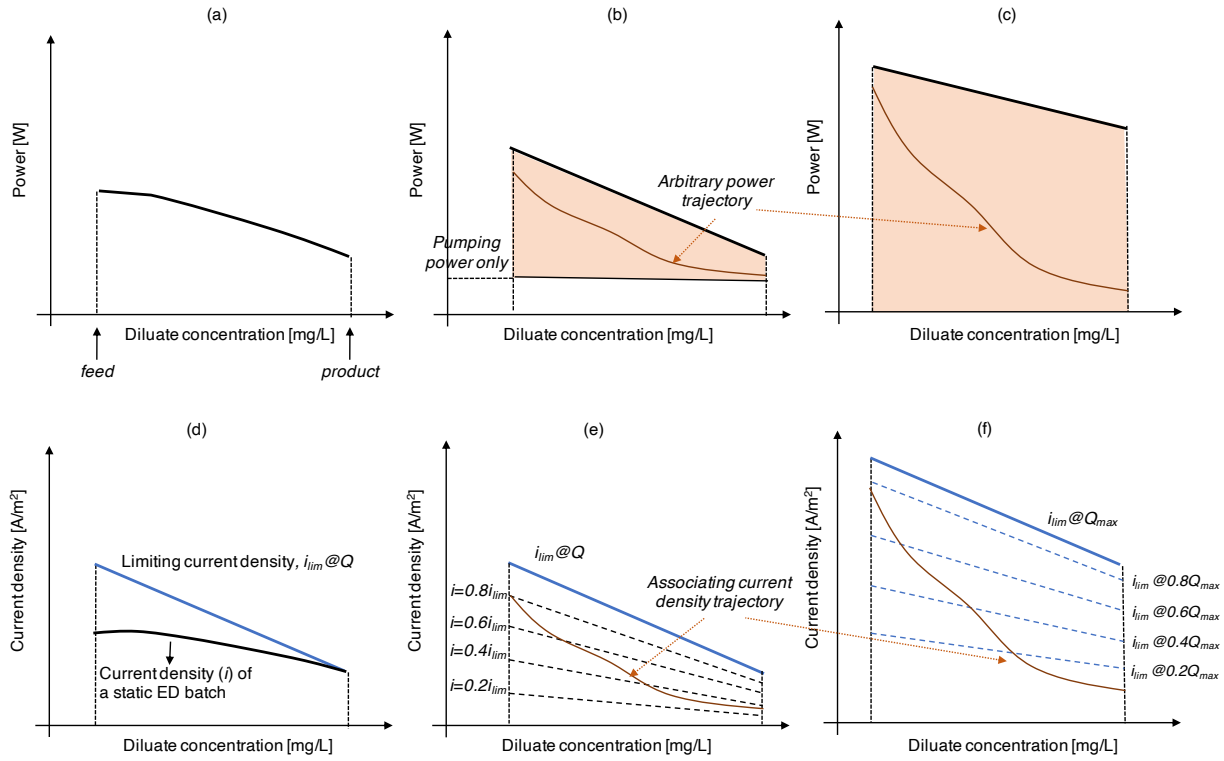


Figure 2: The operational domains of static, voltage-controlled, and voltage- and flow-controlled ED batch operations. (a) The power curve of a conventional static ED batch process (solid line). (b) The flexible power domain of a voltage-controlled ED batch process with constant flow rate (shaded area). (c) The flexible power domain of a voltage- and flow-controlled ED batch process (shaded area). (d) Applied current density and limiting current density of a conventional static ED batch process. The solid black line shows how applied current density changes over a batch as the diluate concentration is reduced. (e) The flexible operational domain of the current density for a voltage-controlled ED batch process with constant flow rate. The dashed lines show ratios of applied current density to limiting current density. (f) The flexible operational domain of the limiting current density for a voltage- and flow-controlled ED batch process. The dashed lines show limiting current densities at varying flow rates. The shaded regions in each plot show the operational domains where a batch ED process could be operated. In b and c, an arbitrary trajectory of a variable power source is shown, with the corresponding applied current density trajectory to produce water shown in e and f, respectively. i_{lim} and i are limiting current density and applied current density, respectively. Q is flow rate. Q_{max} is the flow rate corresponding to maximum power utilization in voltage- and flow-controlled ED operation.

than the maximum possible.

Voltage-controlled ED creates an additional degree of freedom in control by changing voltage applied to the ED stack to manipulate the applied current density. This functionality can be used to either maximize water production by setting the current density always close to limiting (as proposed by Shah et al. [25]), or to maximize utilization of variable power by actively controlling the current density between zero and limiting. In a voltage-controlled batch ED operation with a constant flow rate, the maximum ED power (associated with the electrical field for removing, details in Section 3) is determined by the ED operation at the highest current density, i.e. limiting current density; the pumping power in a voltage-controlled ED system, as presented by Shah et al., is constant. The flexible power range of this sys-

tem is illustrated in Fig. 2b. Any power trajectory in the flexible power range (Fig. 2b) can be met by varying the current density during desalination via voltage control (Fig. 2e). Although a voltage-controlled ED system can be operated in a flexible domain, the applied current density may be substantially lower than limiting due to power restrictions imposed by a variable power source (Figs. 2b and e). Therefore, voltage-controlled operation may also underutilize the ED membranes to produce water.

To simultaneously co-maximize water production per unit membrane area and variable power utilization, control over a second degree of freedom – flow rate – is proposed. Adding flow control enables an ED system to actively vary its limiting current density, in addition to varying the applied current density via voltage control.

Under this control scheme, the flow controller would optimally set the flow rate to set the appropriate limiting current density to fully utilize available power (as illustrated by the dotted lines in Fig. 2f, details can be found in Section 3). At the same time, the voltage controller would ensure the ED system was operating near the “flow-controlled” limiting current density for fully utilizing the membrane capacity. Therefore, voltage- and flow-controlled ED can always maximize water production rate while fully utilizing a variable power resource. Furthermore, as illustrated in Fig. 2c), the upper boundary of power consumption in voltage- and flow-controlled ED can be much higher than in static ED or voltage-controlled ED for a given system size, as increasing flow rate increases limiting current density and the power threshold. Note in Fig. 2c) that the power domain can be reduced to zero by slowing the pumping flow rate to zero.

3. Model-based controller for voltage- and flow-controlled ED batch operation

This section presents a control strategy in which water production and variable power utilization are co-maximized using two degrees of freedom in the ED system - the voltage and flow rate. Water production rate, which is dependent on desalination rate, is maximized by adjusting the voltage at each time step such that the applied current density is maximized without exceeding the limiting current density. Variable power utilization is maximized by adjusting the flow rate at each time step such that the power consumed closely follows the power available from the source.

In our prior work, a robust ED static-operational model was proposed and validated [27]. This model parametrically describes the mass flow and power transfer between components (e.g., ED stack, pumps, etc.) and was demonstrated on multiple sizes of ED systems. This model is used herein to develop the time-variant ED control theory.

The static ED model is first discretized temporally into multiple controlling time steps, τ_i , each of which can be assigned a varying voltage and flow rate. At each time step, the ED operation starts with a bulk diluate concentration, $C_{d,0}^{b,\tau_i}$, and a bulk concentrate concentration, $C_{c,0}^{b,\tau_i}$, at the point between each respective tank and the ED stack inlets (illustrated in Fig. 3a). When a voltage is applied, a concentration boundary layer of thickness δ within a flow channel in the ED stack extends from the membrane surfaces, where the concentration is $C_{d/c,y}^{AEM/CEM,\tau_i}$, to the bulk flow, where the concentration

is $C_{d/c,y}^{b,\tau_i}$. The scripts b , AEM , CEM , d , and c designate bulk flow, the boundary layers near the AEM or CEM membrane, and the diluate or concentrate streams, respectively. The subscript y denotes the location along the discretized flow path, with Y the total discretized flow segments.

The ion increase/removal rate of concentrate/diluate is controlled by varying the voltage, V^{τ_i} , and the flow rates of the concentrate and diluate streams, $Q_c^{\tau_i}$ and $Q_d^{\tau_i}$, respectively:

$$\left(\frac{dC_{d,y}^b}{dt}\right)^{\tau_i} = \frac{1}{NV_y^{cell}} [Q_d^{\tau_i} (C_{d,y-1}^b - C_{d,y}^b)^{\tau_i} - \frac{N\phi I_y^{\tau_i}}{zF} + \frac{NA_y D^{AEM} (C_{c,y}^{AEM} - C_{d,y}^{AEM})^{\tau_i}}{l^{AEM}} + \frac{NA_y D^{CEM} (C_{c,y}^{CEM} - C_{d,y}^{CEM})^{\tau_i}}{l^{CEM}}], \text{ and} \quad (1)$$

$$\left(\frac{dC_{c,y}^b}{dt}\right)^{\tau_i} = \frac{1}{NV_y^{cell}} [Q_c^{\tau_i} (C_{c,y-1}^b - C_{c,y}^b)^{\tau_i} + \frac{N\phi I_y^{\tau_i}}{zF} - \frac{NA_y D^{AEM} (C_{c,y}^{AEM} - C_{d,y}^{AEM})^{\tau_i}}{l^{AEM}} - \frac{NA_y D^{CEM} (C_{c,y}^{CEM} - C_{d,y}^{CEM})^{\tau_i}}{l^{CEM}}], \quad (2)$$

where V_y^{cell} is the volume of each segment, z is the ion charge, F is Faraday’s constant (96,485 C/mol), N is the number of cell pairs, I is the current, ϕ is the current leakage factor, A is the membrane area, $D^{AEM/CEM}$ is the diffusion coefficient in the AEM and CEM membranes, respectively, and l is the thickness of membranes.

The diluate and the concentrate streams flow out from the ED stack and mix with the water in the diluate and concentrate tanks, respectively. The rate of concentration change in the diluate and concentrate tanks can be described as

$$\left(\frac{dC_{d,0}^b}{dt}\right)^{\tau_i} = \frac{Q_d^{\tau_i}}{V_d^{tank}} (C_{d,Y}^{b,\tau_i} - C_{d,0}^{b,\tau_i}), \text{ and} \quad (3)$$

$$\left(\frac{dC_{c,0}^b}{dt}\right)^{\tau_i} = \frac{Q_c^{\tau_i}}{V_c^{tank}} (C_{c,Y}^{b,\tau_i} - C_{c,0}^{b,\tau_i}), \quad (4)$$

where $C_{d,0}^b$ and $C_{c,0}^b$ are the concentrations of the diluate and concentrate tanks (and ED stack inlets), respectively, and V_d^{tank} and V_c^{tank} are the volumes of the diluate and

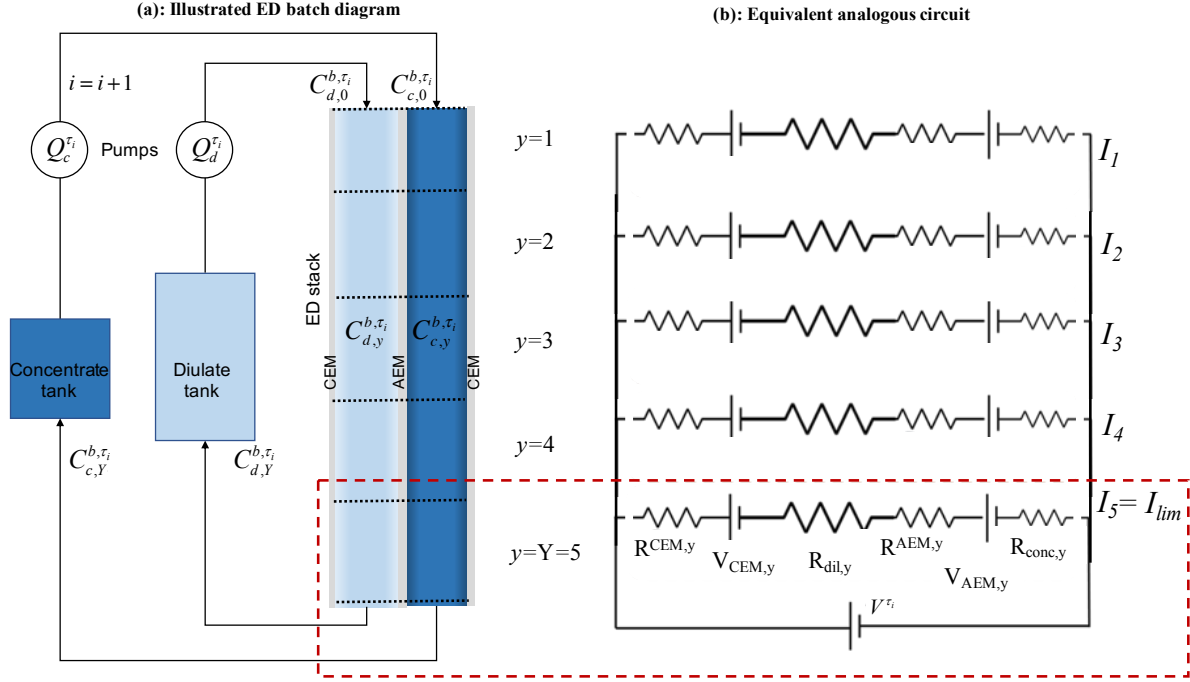


Figure 3: The illustrated flow of the diluate and the concentrate streams in an ED batch system with the associated electrical circuit model used to simulate time-variant ED operation. (a) The two streams in a batch ED system. For every control time step (τ_i), $Q_d^{\tau_i}$, $Q_c^{\tau_i}$, and V^{τ_i} represent the flow rate for the diluate, concentrate, and the voltage, respectively. The simulation model is described starting from the inlet of the stack to the outlet of the tanks, where the time step is updated ($i = i + 1$). C_d and C_c denote the concentration of the diluate and the concentrate, respectively. $y = 1, 2, \dots, Y, Y + 1$ denote segment locations along the flow path. (b) The equivalent electrical circuit for the ED stack. The dashed line represents one segment (one value of y) and its equivalent circuit model. $R^{AEM,y}$ and $R^{CEM,y}$ are the area resistances associated with the AEM and CEM membranes, respectively. $V_{AEM,y}$ and $V_{CEM,y}$ are the potentials across the AEM membrane and the CEM membranes, respectively. $R_{d,y}$ and $R_{c,y}$ are the area resistances associated with the AEM and CEM membranes, respectively. I is the current flowing through the ED stack. I_{lim} is the current when the applied current density equals to the limiting current density.

concentrate tanks, respectively. The desalination rate of the ED system is the desalination rate of the diluate tank, given by Eq. 3.

To calculate the total current, the ED stack is modeled as an analogous DC circuit (Fig. 3b), with a current flowing through each discretized segment

$$I_y^{\tau_i} = \phi_A \left(\frac{WL}{Y} \right) i_y^{\tau_i}, \quad (5)$$

where W is the stack width, L is the membrane channel length, ϕ_A is the open area porosity of the turbulence-promoting channel spacer, and i is the current density. The equivalent circuit elements for each discretized segment are connected in parallel, and thus the voltage is equal across all segments.

To maximize the desalination rate at a given flow rate, the segment current should be maximized, as indicated by Eq. 1. The limiting current density determines the maximum applied current density that can be supported by the ED system before splitting water occurs, as dis-

cussed in Section 2. It can be approximated as a function of the bulk diluate concentration with

$$i_{lim,y}^{+,-} = \frac{zFkC_{d,y}^b}{t_{AEM,CEM}^{+,-}}, \quad (6)$$

where $t^{+,-}$ is the minimum of the dimensionless anion (-) and cation (+) transport numbers in the bulk solution, $t_{AEM,CEM}^{+,-}$ are the transport numbers of the AEM and CEM membranes, respectively, and k is the mass transfer coefficient. k can be represented as

$$k = \frac{ShD_{aq}}{d_h}, \quad (7)$$

where D_{aq} is the diffusion coefficient of the aqueous solution, d_h is the hydraulic diameter, and Sh is the Sherwood Number. Sh represents the mass transfer performance, and is correlated with the Reynolds number and the Schmidt number. These relationships are described further in Appendix A.

As indicated by Eq. 6, the limiting current density is proportional to the bulk diluate concentration. As the voltage increases, the applied current density of the last segment ($y = Y = 5$) is the first to reach the limiting current density because the bulk diluate concentration at the outlet is the lowest within the ED stack. Thus, the maximum voltage that can be applied without exceeding the limiting current density is the voltage when the applied current density of the last segment is close to the limiting current density. This maximum voltage is

$$V^{\tau_i} = V_{el} + N(V_Y^{CEM} + V_Y^{AEM}) + Nr_i i_{lim,Y} (R_{d,Y} + R_{c,Y} + R_Y^{BL} + R^{AEM,Y} + R^{CEM,Y}), \quad (8)$$

where: V_{el} is the electrode potential (1.4 V when hydrogen ions are reduced at the cathode and chloride ions are oxidized at the anode); $V_{CEM,Y}$, $V_{AEM,Y}$ are the potentials across the CEM and AEM membranes, respectively; R_Y^{BL} , $R^{AEM,Y}$, $R^{CEM,Y}$ are the area resistances associated with the concentration boundary layers, the AEM membranes, and CEM membranes, respectively; and r_i is the safety factor for approaching the limiting current density. r_i provides an additional degree of freedom to track (with an appropriate safety-margin) the limiting current density throughout the batch process [26]. $R_{d,Y}$ and $R_{c,Y}$ are the resistances associated with the diluate and concentrate streams, respectively, which can be further represented as

$$R_{d,Y} = R_{d,Y}^b + R_{d,Y}^{AEM} + R_{d,Y}^{CEM}, \text{ and} \quad (9)$$

$$R_{c,Y} = R_{c,Y}^b + R_{c,Y}^{AEM} + R_{c,Y}^{CEM}, \quad (10)$$

where $R_{d/c,Y}^b$ is the resistance of the bulk flow, and $R_{d/c,Y}^{AEM}$ and $R_{d/c,Y}^{CEM}$ are the resistances in the boundary layers near the membrane surfaces, respectively. These equivalent resistances depend on the diluate and concentrate concentrations; detailed derivations for these resistances can be found in Wright et al. [27].

The potentials associated with the concentration difference across the exchange membranes, $V_{AEM,Y}$ and $V_{CEM,Y}$, can be approximated by

$$V_{AEM,Y} = \frac{(2t^{AEM} - 1)RT}{F} \log\left(\frac{\gamma_c C_{c,Y}^{AEM}}{\gamma_d C_{d,Y}^{AEM}}\right), \text{ and} \quad (11)$$

$$V_{CEM,Y} = \frac{(2t^{CEM} - 1)RT}{F} \log\left(\frac{\gamma_c C_{c,Y}^{CEM}}{\gamma_d C_{d,Y}^{CEM}}\right), \quad (12)$$

where T is the temperature and R is the gas constant, $8.31JK^{-1}mol^{-1}$ [27].

To maximize variable power utilization, total system power consumption is adjusted to closely follow the input power. The total system power consumption of a time-variant ED system is estimated by summing the power consumption of the most power-consuming components, which are the DC power supply for the ED stack and the diluate and concentrate pumps:

$$P_{total}^{\tau_i} = P_{ED}^{\tau_i} + P_{pump,d}^{\tau_i} + P_{pump,c}^{\tau_i} \quad (13)$$

where $P_{pump,d}$ and $P_{pump,c}$ denote the power consumed by the diluate pump, and the concentrate pump, respectively. P_{ED} denotes product of the voltage and current applied to the ED stack.

The power consumed by the variable speed pumps of the diluate and concentrate streams will depend on the flow rate and the hydraulic characteristics of the full ED system. In general, the power consumption of a variable speed-controlled centrifugal pump follows the Affinity Laws (also known as ‘‘the Pump Laws’’) [28],

$$\frac{Q_{d/c}^{\tau_i}}{Q_{ref}} = \frac{n_{d/c}^{\tau_i}}{n_{ref}}, \quad (14)$$

$$\frac{H_{d/c}^{\tau_i}}{H_{ref}} = \left(\frac{n_{d/c}^{\tau_i}}{n_{ref}}\right)^2, \text{ and} \quad (15)$$

$$\frac{P_{pump,d/c}^{\tau_i}}{P_{ref}} = \left(\frac{n_{d/c}^{\tau_i}}{n_{ref}}\right)^3, \quad (16)$$

where n is pump speed and H is the pump head. Q_{ref} , H_{ref} , P_{ref} , and n_{ref} indicate the referenced operation points of the system.

The power consumption of the DC power supply in an ED stack (i.e. the desalinating power) is estimated as the product of the current and the applied voltage,

$$P_{ED}^{\tau_i} = (VI)^{\tau_i}. \quad (17)$$

To match the instantaneous power input, the instantaneous power consumption of the ED system, $P_{total}^{\tau_i}$, is controlled by varying the voltage and flow rate. As shown by Eq. 14 and Eq. 16, the pumping power explicitly depends on the flow rate, which can be used to estimate the new pumping power when a new flow rate is applied.

To estimate the new desalinating power, $P_{ED}^{\tau_i}$, when a new voltage is applied to the ED stack is non-trivial. It requires summing all of the segments’ currents, as shown in Fig. 3, which requires solving a system of equations,

including Eq. 1 and Eq. 2, at varying flow rates. However, variable power inputs from solar or wind sources, or changes in electricity tariffs in dynamic grid pricing, may vary on the order of seconds, requiring the controller to respond quickly to identify and apply optimal voltages and flow rates. To accelerate the controller's computational efficiency, an explicit method of estimating the ED desalination power under varying flow rate conditions is proposed.

To reduce computation time, the controller only considers electromigration for ion transfer. Electromigration generally contributes $\geq 90\%$ of the mass transfer in ED desalination [27, 29], and the contribution is even higher with a high current (enabled by a high flow rate, as indicated by Eq. 6). This assumption results in the explicit current estimation

$$I_{appr}^{\tau_i} = \frac{Q_d^{\tau_i} (C_{d,0}^b - C_{d,Y}^b)^{\tau_i} zF}{N\phi}, \quad (18)$$

where $I_{appr}^{\tau_i}$ is the approximated current. In this case, the transience of the changing flow rate is negligible compared to the transience of the changing dilute concentration, due to the incompressible nature of water.

Using the approximated current (Eq. 18) and the maximized voltage (Eq. 8), the ED desalination power at the new flow rate can be explicitly estimated (Eq. 17). The total power consumption can then be evaluated at a different flow rate and combined with Eq. 16, which enables the controller to efficiently optimize flow rates to match or closely follow the available variable power input.

Figure 4 shows a flowchart of the final model-based controller, incorporating both desalination rate and power utilization components. By using this controller, water production is maximized by setting a voltage that maximizes the ion transfer rates and avoids water splitting occurring in the stack at a particular flow rate. Then the variable power utilization is maximized by setting the flow rate using an optimization feedback loop that minimizes the difference between the power consumption and the available power input. As a result, this strategy enables the simultaneous maximization of water production and variable power utilization, facilitating the most efficient use of water and available power at every point in time.

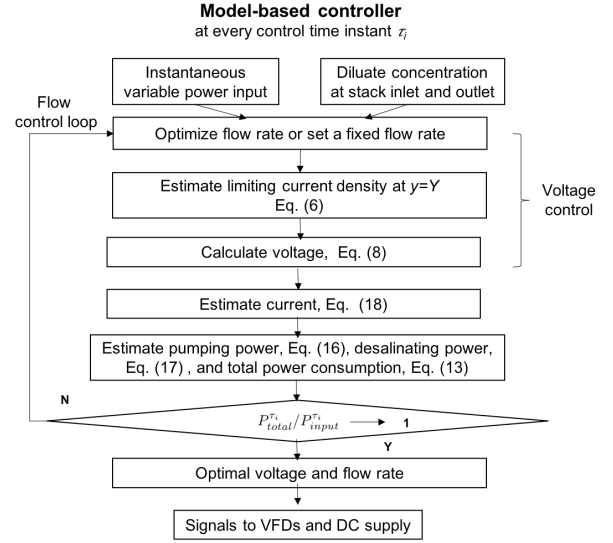


Figure 4: Flowchart of the model-based controller for time-variant ED operation. $P_{total}^{\tau_i}$ and $P_{input}^{\tau_i}$ are the total power consumption (including the ED power and the pumping power) and the variable power input at every control time instant τ_i , respectively. Y refers to the total discretized sections of the ED stack referenced in Fig. 3.

4. Pilot time-variant ED system design

4.1. Experimental setup

A pilot-scale time-variant ED prototype was built to validate the proposed control theory, following the configuration shown in Fig. 5. The ED stack was manufactured by Suez Water Technologies and Solutions (Model AQ3-1-2-50-35), with the parameters listed in Table 1. Two pumps (Xylem Goulds 3SV-11) recirculated the diluate and concentrate streams with their speed controlled by pump controllers (Xylem CentriPro Aquavar). A 60-25V DC supply (TDK-Lambda GEN) supplied the voltage (regulated to $\pm 1\%$ of the commanded value). The polarity of the applied voltage was reversed between batches by switching the diluate and concentrate channels in the stack using valves. This reversal operation has been shown to reduce the scaling propensity in ED desalination [30].

Two flow meters (Omega FP1408) were used to monitor the flow rate ($\pm 1\%$) in the diluate and concentrate streams. In-line conductivity probes (Connectivity Instruments CDCE-90) interfacing with conductivity controllers (Connectivity Instruments CDCN-91) monitored the conductivity (to an accuracy of $\pm 2\%$) at the entry and exit of the ED stack. All sensors interfaced with a CLICK I/O Programmable Logic Controller (PLC) with analog input and output modules (C0-04AD-1, C0-04AD-2, and C0-04DA-2). Each electrode was rinsed

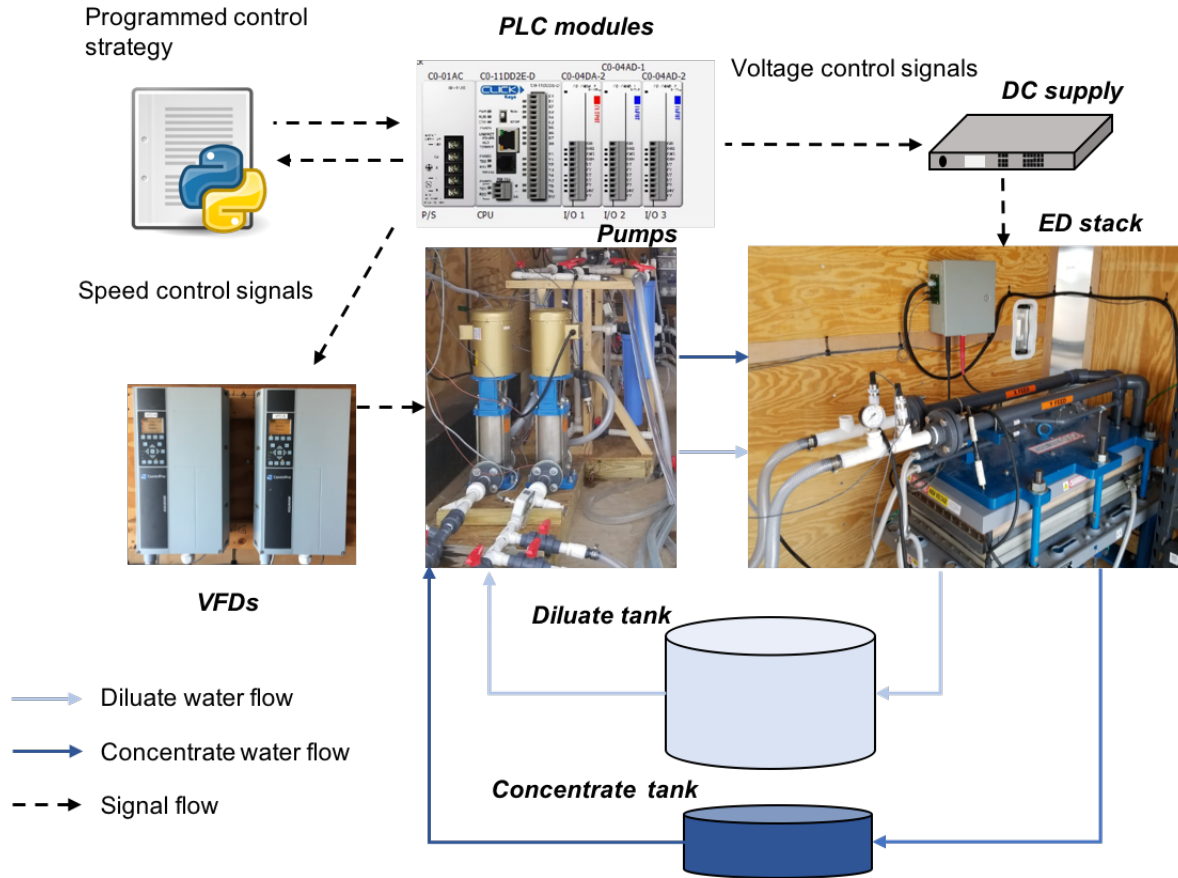


Figure 5: Major system elements and their interactions for the time-variant ED prototype tested at the Brackish Groundwater National Desalination Research Facility (BGNDRF) in Alamogordo, New Mexico.

Design Variables	Value
ED cell pairs	30
Diluate tank volume, m ³	0.42 ±4%
Brine tank volume, m ³	0.28 ±7%
Flow Path Width, cm	19.7
Flow Path Length, cm	168
AEM Resistance, Ω cm ²	7
CEM Resistance, Ω cm ²	10
Void fraction	0.83±0.03
Area porosity	0.70±0.02
Spacer thickness, mm	0.71±0.01

Table 1: Parameters of the ED stack

475 with a sodium sulfate solution (conductivity over 14
476 mS/cm ±2%) held at a flow rate of 6-8 LPM (±1%).

477 Feed water was taken from Well No. 1 at the Brackish
478 Groundwater National Desalination Research Facility (BGNDRF) in Alamogordo, New Mexico. Major
479

480 constituents in the water are listed in Table 2. The feed
481 water salinity was similar to that of a previous pilot-scale
482 PV-ED field study conducted by our group in rural India [12]. Water quality measurements were performed
483 by DHL Laboratories (San Antonio, TX). In each batch
484 reported in the following section, the feed water was desalinated to a target product concentration of 500 μS/cm
485 with a batch size of 0.42 m³.
486
487

4.2. Controller implementation

488 The pump speeds and voltage applied to the ED stack
489 electrodes were controlled by variable frequency drives
490 (VFDs) and a programmable DC power supply according
491 to the received control signals from the implemented
492 controller script, respectively. The controller strategy,
493 implemented in Python, calculated an optimal voltage
494 and flow rate using real-time measurements of variable
495 power inputs and conductivity from both the diluate and
496 concentrate streams, based on the model introduced in
497

Parameters	Value
Na^+ , $mg L^{-1}$	293 ± 29
Mg^{2+} , $mg L^{-1}$	12.6 ± 1.3
Ca^{2+} , $mg L^{-1}$	54.6 ± 5.5
Cl^- , $mg L^{-1}$	38.1 ± 3.8
SO_4^{2-} , $mg L^{-1}$	504 ± 50
Alkalinity Bicarbonate, $mg L^{-1}$ as $CaCO_3$	161 ± 1
Total dissolved solids (TDS), $mg L^{-1}$	995 ± 72
Conductivity, $\mu S cm^{-1}$	$1,500 \pm 30$

Table 2: The major constituents in the brackish groundwater from Well NO.1 at the Brackish Groundwater National Desalination Research Facility (BGNDRF), measured on 3-Dec-2018.

Section 3. Pump performance curves were experimentally generated from the two installed pumps based on measurements at multiple speeds. Speed versus flow and speed versus power pump curves were empirically fit to the experimental data and used in the controller implementation, as described in Section 3. The fitted pump curves are plotted in Appendix B.

Control signals were applied to the time-variant ED prototype in an open loop. Communication between the controller script and modules in the prototype was implemented via PLC modules. Using measured concentrations at the current time, controller predictions were used to optimize the flow rate and voltage. Signals for these values were then sent to the VFDs and the DC power supply to control the flow rate and voltage, respectively, for the upcoming time step. The duration of the time step was 3 s, based on preliminary testing and chosen to capture variations in the power input while allowing enough time for the ED system to reach a new steady state after the latest change in voltage and flow rate. The system response time was determined experimentally. The same time step of 3 s was used for simulation studies.

5. Pilot time-variant ED system testing and results

5.1. Controller test for variable voltage, high constant flow rate ED

The efficacy of the control theory presented in Section 3 was first tested with a fixed, high flow rate and variable voltage to see if the controller could produce an increased desalination rate compared to static ED operation. The maximum flow rate in an ED system depends on many factors and is determined by the maximum pump speed. In this study, the maximum linear velocity

in the membrane channels was restricted to be ~ 20 cm/s ($\pm 1\%$), corresponding to 42 LPM bulk flow rate. This is already significantly higher than the velocity in the membrane channels of conventional static ED operation (4-12 cm/s) [25], which is set to ensure operational stability of the membranes and spacers. Figure 6 shows the current, power consumption, and diluate conductivity over a batch for voltage-controlled ED operation at the maximum flow rate of 42 LPM. Static ED operation with a flow rate of 25 LPM (~ 12 cm/s in the membrane channels) is shown for comparison. In these tests, the current density was not allowed to exceed 70% of limiting (which is a function of flow rate, described in Section 3).

Figure 6 demonstrates that running the time-variant ED prototype at a high flow rate increased the operational domain (shaded region) compared to the single operating trajectory for static ED (black line), achieving a 45% increase in desalination rate (Fig. 6c). Further comparisons of static ED to time-variant ED at different flow rates are shown in Appendix C. The controller predictions and the experimentally measured current and power were consistently aligned (within 1.5% RMS error). This indicates that the controller can accurately predict current and then successfully predict power consumption. The results in Fig. 6 show that the controller could enable the time-variant ED system to directly use variable power sources over a wide range of operating conditions by varying flow rate and ED stack voltage, as discussed in Section 3.

5.2. Controller test for voltage- and flow-controlled ED

To further characterize the performance of voltage- and flow-controlled ED operation, and validate the control theory presented in Section 3, the time-variant ED prototype system was run using a representative solar power input profile (Fig. 7a) during one batch. The solar profile was recorded by a set of local solar panels (Hyundai HiS-S285RG) at BGNDRE. The target product concentration was set to $300 mg L^{-1}$ ($\sim 500 \mu S cm^{-1}$) for this test. The controller was able to command the prototype ED system to consumer power on a trajectory that closely followed (within 10.0% RMS error) the reference solar power profile (Fig. 7a) while maintaining a measured product water concentration of $300 mg L^{-1}$. These results demonstrate the ability of the time-variant ED system to adaptively desalinate water to a desired product concentration while adjusting voltage and flow rate to match an arbitrary variable power level. This flexibility could allow the time-variant ED system to directly integrate with real clean energy sources, such as solar or wind, without requiring significant battery capacity.

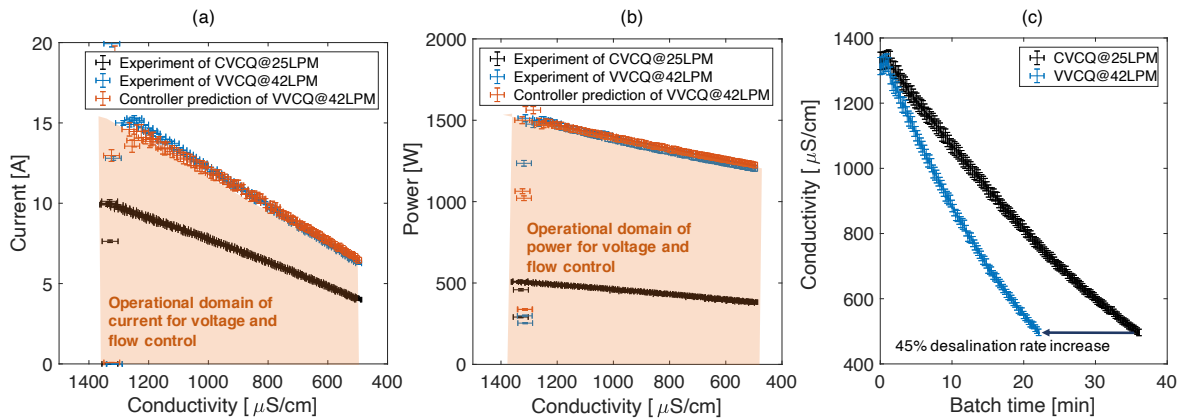


Figure 6: Controller predictions and experimental ED batch performance under voltage-controlled variable voltage (VV) and high constant flow rate (CQ) (42 LPM) conditions versus constant voltage (CV), moderate constant flow rate (CQ) (25 LPM) conditions. Results are presented for: (a) current versus diluate conductivity; (b) total power of the ED system versus diluate conductivity; and (c) diluate conductivity versus batch time (experimental performance only). The shaded regions in (a) and (b) represent the flexible operational domain for which a flexible ED system could operate using direct power from a variable power source.

582 Figure 7b shows the controlled power consumption
 583 profile of the pilot-scale time-variant ED system while
 584 the controller was fed three arbitrary constant input
 585 power levels of 1000 W, 850 W, and 730 W. Constant
 586 power levels were chosen as inputs for three primary
 587 reasons. First, any variable power source can be approx-
 588 imated as constant for a very short duration. Second,
 589 at each controlling time step (every 3 s in these exper-
 590 iments), the controller needs to optimize and adjust
 591 voltage and flow rate to match a singular power value;
 592 whether this value changes in time or not is arbitrary in
 593 the perspective of the controller. To maintain a constant
 594 power consumption, the controller has to continuously
 595 make adjustments, just as it would to follow a variable
 596 input power profile. Third, operating a constant power
 597 while maximizing water production rate simulates real-
 598 world situations where power consumption would have
 599 to be maintained under a threshold, say within the speed
 600 limitations of a wind turbine or in an industrial grid-
 601 powered application where there are different charge
 602 rates depending on power draw. Therefore, the three
 603 constant power levels were used to robustly test the load
 604 flexibility of the prototype time-variant ED system and
 605 demonstrate the utility of the control model.

606 The results in Fig. 7b demonstrate that the controlled
 607 time-variant ED system power consumption was able to
 608 closely match the predefined constant input power levels
 609 for all three cases; the RMS errors for each test were
 610 1.7% for 1000 W, 4.2% for 850 W, and 6.3% for 730 W,
 611 as the batch desalinates from 1400 $\mu\text{S}/\text{cm}$ to about 500

$\mu\text{S}/\text{cm}$. All of the time-variant ED operations had higher
 612 desalination rates (ranging from 6-15%) than the static
 613 ED process used as a benchmark (Fig. 7c). The shaded
 614 regions in Figs. 7a and b show how much flexibility
 615 remains in the operational domain, with the upper limit
 616 bounded by the same maximum power conditions shown
 617 in Fig. 6, defined by variable voltage operation and a
 618 constant pumping flow rate of 42 LPM.
 619

5.3. Desalinating and pumping power

620 Although the time-variant ED batch trajectories
 621 largely align with their respective input power profile,
 622 there are some small deviations. Particularly in the
 623 cases with relatively low power input, the measured ex-
 624 perimental power tends to fluctuate around the variable
 625 power input. To explore this deeper, the data from Fig.
 626 7b were decomposed to analyze the power contributions
 627 from the ED desalination process and pumping.
 628

629 Figure 8 shows that the measured and predicted ED
 630 desalination power values follow the same trends for the
 631 three tested cases. However, for power levels of 850
 632 W and 730 W, the measured total desalination power
 633 is slightly under the predicted power. These deviations
 634 are likely due to the neglected back diffusion through
 635 the membranes into the channels; because the controller
 636 does not take back diffusion into account, it tends to
 637 predict a higher current for a given applied voltage (Eq.
 638 18). The power becomes increasingly over-predicted at
 639 lower flow rates because the back diffusion is higher, as
 640 seen in the 850W and 730W cases.

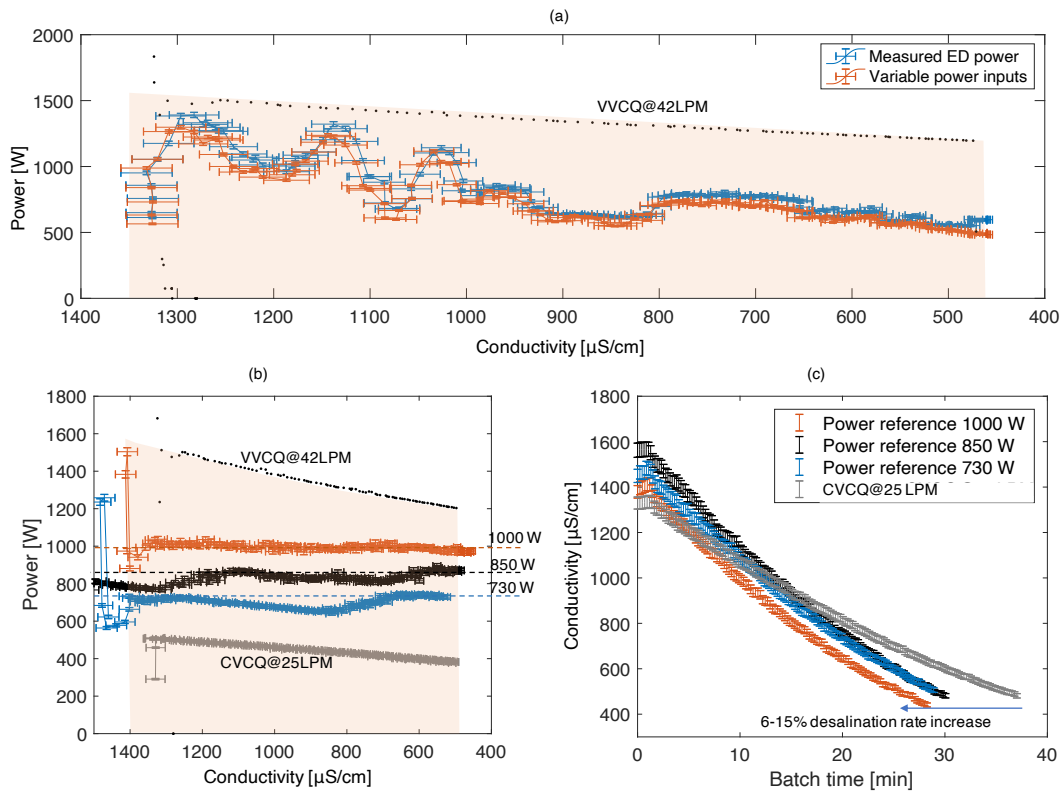


Figure 7: Time-variant ED system performance for varying power inputs. (a) Measured power usage for time-variant voltage- and flow-controlled ED operation from the pilot-scale ED prototype while following a representative, measured solar power profile during one batch. (b) Measured power consumption for time-variant voltage- and flow-controlled ED operation from the pilot-scale ED prototype under three constant power inputs (1000 W, 850 W, and 730 W) during one batch. (c) The corresponding conductivity profiles from the results in (b). A benchmark constant voltage, constant flow rate static ED batch (CVCQ) process at 25 LPM flow rate is shown for comparison in (b) and (c). To demonstrate the operational limits at maximum pumping power, a variable voltage, constant flow rate ED batch process (VVCQ) at 42 LPM is shown in (a) and (b), which marks the upper boundary of the operational domain (shaded region).

641 The measured pumping power follows the general
 642 trend of the predicted pumping power in all of the tested
 643 cases, with the exception of some small fluctuations in
 644 the 850 W and 730 W cases (Figs. 8b and c, respec-
 645 tively). The small fluctuations at lower input power
 646 levels may be caused by the behavior of the pump when
 647 operating outside its intended performance curve. The
 648 applied voltage and flow rate in the three cases are plot-
 649 ted in Figs. 9a and b, respectively. The pumps used in
 650 the prototype ED pilot have their highest efficiency at
 651 flow rates of 40-70 LPM. Figure 9b plots the flow rate
 652 for each input power level during the ED batch. The
 653 pumps were operated in a region outside their intended
 654 performance curve for the lower power levels of 850 W
 655 and 730 W, where they would be expected to perform
 656 less predictably and stably. They were operated closer
 657 to their high efficiency operation zone at the power level
 658 of 1,000 W. A slightly downsized pump may have im-

proved the power fluctuations seen in Fig. 8. In spite of
 these small fluctuations, the measured pumping power
 closely followed the values predicted by the controller
 (to within 1.8% RMS for 1000 W, 4.6% RMS for 850
 W, and 5.7% RMS for 730 W, as the batch desalinates
 from 1400 $\mu\text{S}/\text{cm}$ to about 500 $\mu\text{S}/\text{cm}$).

A large spike in the voltage is apparent in Fig. 9a at
 the beginning of each batch for all three power levels,
 accompanied by a rapid drop in flow rate just before the
 voltage spike. These features are caused by an under-
 prediction of current at the beginning of the batch by
 the controller. At this moment, the electric potential is
 instantaneously applied across the membranes in the ED
 stack. In a real stack, for the initial diluate concentra-
 tion in the membrane channels to be perturbed by the
 electrical field, salts must accumulate before building
 up concentration variations between the inlet and outlet.
 These transient effects are ignored by the controller, and

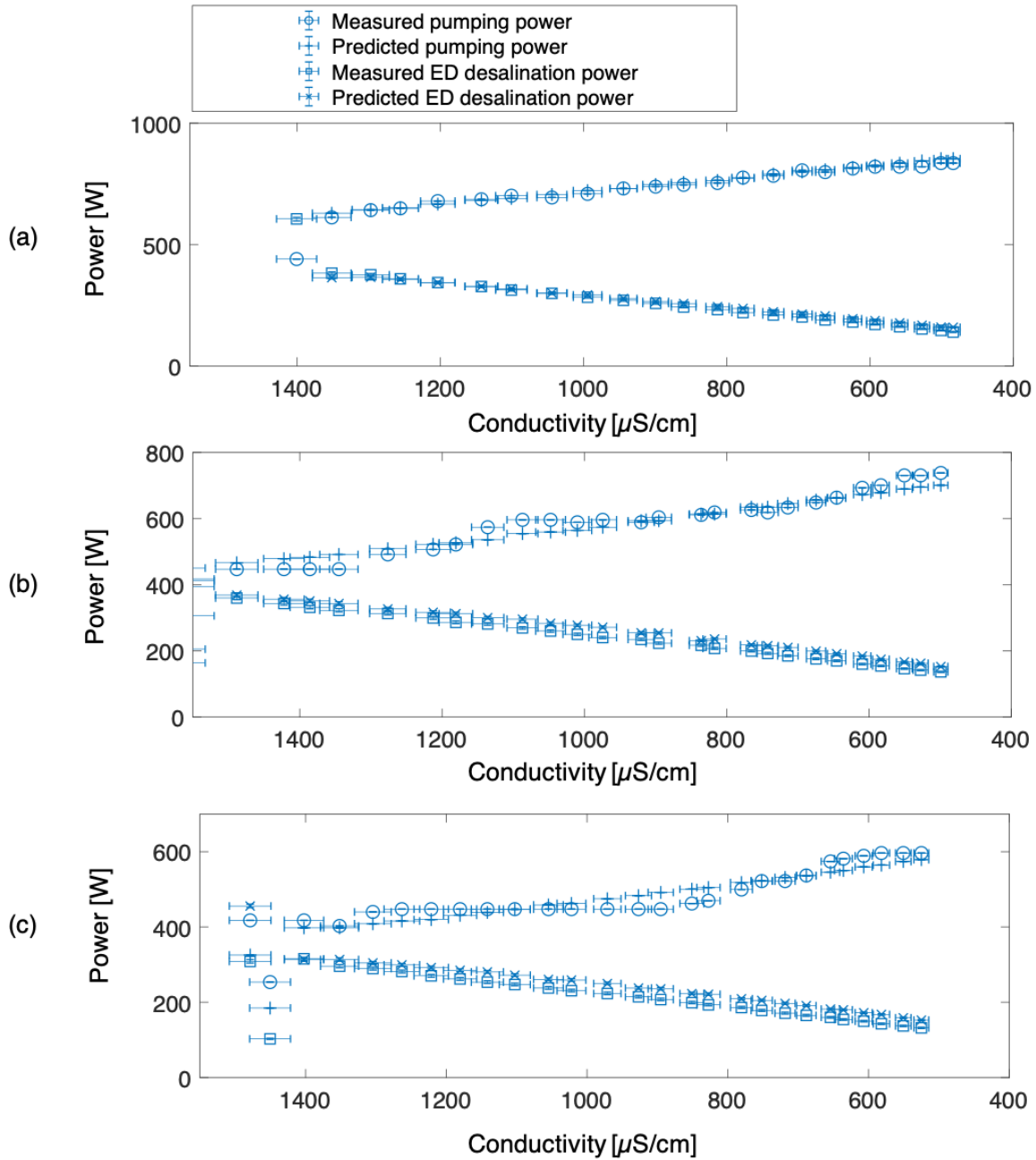


Figure 8: Experimentally measured power consumption of the pump and the ED desalination process, and the controller predictions for reference power inputs of (a) 1000 W, (b) 850 W, and (c) 730 W.

677 therefore, the approximated current from Eq. 18 under-
 678 estimates the applied current at this moment, causing
 679 an overprediction of flow rate in the first few instants,
 680 as seen in Fig. 9b. After the voltage spike, the con-
 681 centration drop across the diluate stream becomes fully
 682 developed and the effect of the accumulating salts be-

comes insignificant. During this transient period, the
 control model has a large error (compared to the period
 after the spike) due to the assumptions used in the model
 being briefly invalid. Therefore, for this short duration,
 a small amount of battery energy storage is required to
 supply enough power. This transient period is generally

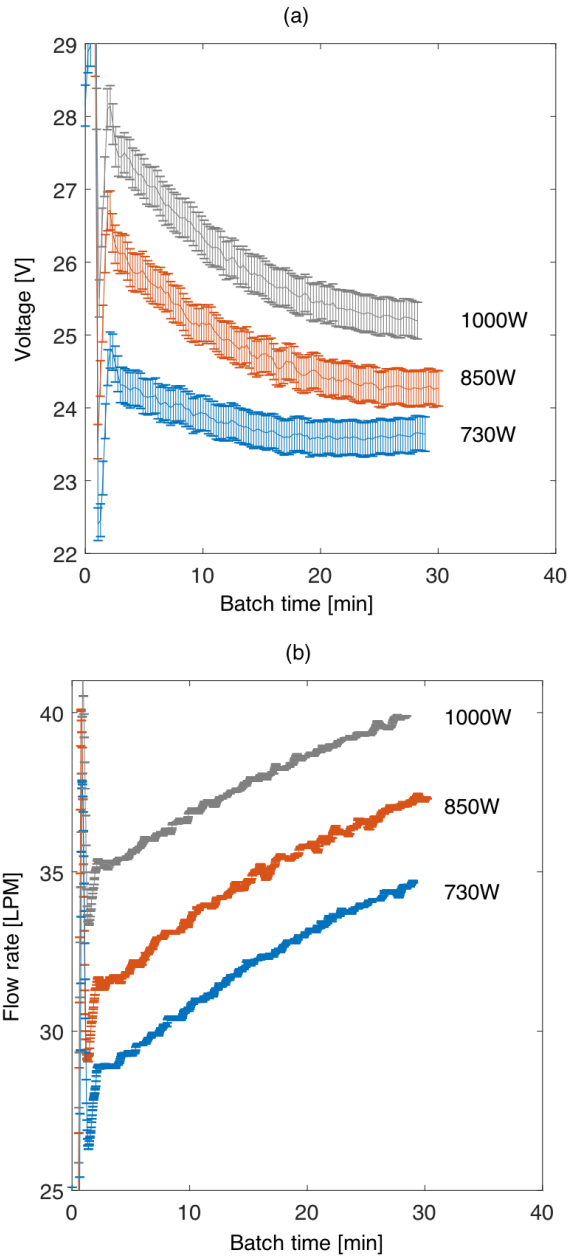


Figure 9: Experimentally measured voltage and flow rates during time-variant ED operation with reference power inputs of (a) 1000 W, (b) 850 W, and (c) 730 W.

689 very short (less than 1 min per 25-40 min batch in the
 690 pilot system), and the required battery capacity is nearly
 691 negligible. For example, for the pilot time-variant system
 692 presented herein that requires batteries for reshaping
 693 power over ~ 1 min, the required battery capacity could
 694 be as small as 1/40-1/25 the required battery capacity
 695 of traditional renewable-powered ED systems that use

batteries to reshape the variable power input throughout
 the batch.

5.4. The trade-off between production rate and energy consumption

Although voltage and flow rate follow the same trends in variation across the three input power levels shown in Fig. 9, they differ in magnitude. Higher power levels tend to have higher flow rates and higher voltages. Comparing pumping power consumption in Fig. 8 with ED stack voltage in Fig. 9a, the pumping power varies significantly with varying voltage in each of the three power levels, but the measured ED desalination power does not. This indicates that the scaling factors for flow-to-power and voltage/current-to-power differ. Because the feed concentration ($\sim 1500 \mu\text{S cm}^{-1}$) in each case is desalinated to a same product concentration ($\sim 500 \mu\text{S cm}^{-1}$), the electrical resistances (Eqs. 9 and 10) of both the concentrate and the diluate streams should be similar, independent of case. As a result, the ED desalination power primarily scales with V^2 , according to Eq. 17. In contrast, the pumping power scales with Q^3 , according to Eq. 16. As a result, the pumping power increases much faster with flow rate, causing the pumping to consume more power than ED in all three test cases. Efficient pumping is therefore critical to improve the energy efficiency of time-variant ED batch operation.

Table 3 gives the specific energy consumption (SEC) and desalination rate for the three time-variant, voltage- and flow-controlled ED batch cases at different power inputs, along with a static ED batch process with a flow rate 25 LPM. The starting feed concentration was slightly different from batch-to-batch during the experiments; each was run with a target product concentration of $500 \pm 5 \mu\text{S cm}^{-1}$. The results in Table 3 indicate the trade-off between SEC and batch time (equivalent to desalination rate in m^3/h) and suggest they are correlated non-linearly. The desalination rate was increased by 29%, 20% and 19% by using 62%, 52% and 30% more energy, respectively, compared to static ED. The pumping SEC also corroborates the significantly increased fraction of energy consumed by pumping compared to ED desalination under higher input powers. The percentage contribution of pumping to SEC increases from 68% in the static ED case to 74% in the time-variant ED case with input power of 1,000 W.

Parameters	CVCQ@25LPM	VVVQ@730W	VVVQ@850W	VVVQ@1000W
Feed concentration [$\mu S/cm$]	1340 \pm 27	1460 \pm 29	1560 \pm 31	1410 \pm 28
Product concentration [$\mu S/cm$]	500 \pm 10	505 \pm 10	500 \pm 10	500 \pm 10
Batch time [min]	35.9 \pm 3.3%	29.0 \pm 3.3%	28.9 \pm 3.3%	25.5 \pm 3.3%
SEC [kWh/m^3]	0.63 \pm 0.03	0.82 \pm 0.04	0.96 \pm 0.05	1.02 \pm 0.05
Pumping SEC [kWh/m^3]	0.43 \pm 0.02	0.56 \pm 0.03	0.68 \pm 0.04	0.75 \pm 0.04
ED desalination SEC [kWh/m^3]	0.20 \pm 0.01	0.26 \pm 0.01	0.28 \pm 0.01	0.27 \pm 0.01
Batch time compared to CVCQ	N/A	82% \pm 5.8%	81% \pm 5.8%	71% \pm 5.8%
SEC compared to CVCQ	N/A	130% \pm 6.8%	150% \pm 7.0%	160% \pm 6.8%
Pumping SEC compared to CVCQ	N/A	130% \pm 7.1%	160% \pm 7.5%	170% \pm 7.1%
ED desalination SEC compared to CVCQ	N/A	130.00% \pm 6.3%	140.00% \pm 6.1%	130.00% \pm 6.2%

Table 3: Performance of the pilot-scale prototype in variable voltage, variable flow (VVVQ), time-variant ED batch operation with constant power inputs of 730W, 850W, and 1000W. Performance of a benchmark constant voltage, constant flow (CVCQ), static ED batch process at a flow rate of 25LPM is given for comparison. All tests were run with a target product concentration of 500 \pm 5 $\mu S cm^{-1}$.

6. Discussion

In this work, the time-variant method for operating a batch ED system has been demonstrated to be load-flexible and able to accommodate variable power sources and maximize the rate of water production, in order to reduce the water cost. This new operational strategy is analogous to how multi-stage ED stacks, or series assemblies of ED stacks, are arranged with different voltages applied to each electrical stage to maintain applied current density near limiting, and different numbers of parallel flow channels to manipulate flow velocity for a desired limiting current density and/or to minimize pumping power [31]. Because time-variant ED batch operation is able maintain applied current density near limiting and fully utilize an available power source for maximized water production rate, ED systems designed with this technology may result in reduced capital costs compared to static, continuous ED systems composed of multi-stage ED stacks or multiple ED stacks in series. The hardware required to make a time-variant ED system is readily available off-the-shelf, with some components (e.g. conductivity sensors) already routinely included in conventional ED batch systems.

Section 5.3 reveals a trade-off between power consumption and desalination rate. Flexible operation allows ED systems to utilize much higher levels of power compared to a similarly sized static ED system, which will increase desalination rate but result in higher SEC. The additional energy consumption of the accelerated production rate may not be an issue in some applications in which operational time is critical, or available energy is abundant (e.g. solar irradiance at mid-day). To be economically viable therefore, the cost of energy provided by either on-grid or off-grid sources should be low enough to justify the additional energy consumption

required to operate time-variant ED systems at the high flow rates required for maximizing desalination rate. For on-grid cases, operation costs could be reduced while maximizing production rate by either limiting the overall system power threshold and/or the pumping power threshold.

To justify higher SEC in on-grid applications, time-variant ED technology could utilize variable electricity tariffs between peak and off-peak times, which are part of a demand response (DR) approach for reducing peak loads [32]. Various DR programs provide financial benefits to customers who are willing to shift loads from peak times to off-peak times. Wang and Li [16] surveyed time-of-use pricing services in the US and found that peak time prices can be 500-600% higher than off-peak time prices in summer months (June-September), and 30%-200% higher in other months. Such considerable price differences could incentivize the adoption of time-variant ED systems to produce more water, or produce water at a faster rate during off-peak periods, than existing technologies, which could potentially reduce overall water costs. Time-variant ED systems could also facilitate the integration of renewable energy sources into the electrical grid by providing a consumer of excess energy production on an irregular schedule, thereby reducing carbon emissions from energy sources currently used to meet peak demands (e.g. coal and natural gas).

For off-grid applications, time-variant operation could enable ED systems to directly utilize all available intermittent renewable energy, such as peak midday solar irradiance that would otherwise be neglected or stored in batteries. This could significantly reduce system capital costs by reducing the battery capacity required for renewable energy peak shifting. Small battery capacity and high water production rates would be particularly valuable for disaster response applications, where

812 small-scale, lightweight, PV-powered time-variant ED
813 systems could be rapidly shipped and deployed. For
814 microgrid solar systems, which are gaining popularity
815 in cost-constrained, remote communities in developing
816 countries [33], time-variant ED systems could reduce
817 electricity costs by utilizing otherwise unused solar en-
818 ergy and creating additional value through the produc-
819 tion of potable water.

820 7. Conclusions

821 This paper proposes a highly-flexible and production-
822 optimized ED desalination technology for brackish wa-
823 ter with two degrees of freedom of control: applied
824 ED stack voltage and pumping flow rate. This control
825 method can enable flexible and effective uses of variable
826 power sources on a timescale of seconds to maximize
827 water production, which has particular value in utilizing
828 renewables (e.g. wind and solar). Additionally, time-
829 variant ED operation can improve utilization of mem-
830 brane area by maximizing the applied current density,
831 which could facilitate smaller and lower-cost desalina-
832 tion systems to hit a target production volume, compared
833 to what can be achieved with static ED operation.

834 A pilot-scale, time-variant ED system was designed
835 and built to validate the theory presented in this work.
836 The time-variant system was able to utilize up to ~3 more
837 power than if operated at static voltage and flow rate,
838 achieving up to 45% greater desalination rates. Within
839 the operational domain, the pilot system was shown to
840 successfully operate at three different power inputs, suc-
841 cessfully adjusting voltage and flow rate as anticipated.
842 A trade-off between SEC and desalination rate was iden-
843 tified; in the three tests with different power levels, de-
844 salination rate was increased by 29%, 20% and 19% by
845 using 62%, 52% and 30% more energy, respectively,
846 compared to static ED batch operation.

847 For on-grid applications, time-variant ED operation
848 could enable water producers to align production time
849 and power consumption favorably with energy tariffs,
850 which are lower in the evening. For off-grid systems,
851 time-variant ED could remove or reduce the need for
852 batteries (and their associated costs) by producing water
853 when energy is available. The technology presented
854 herein may enable engineers to design brackish water
855 ED desalination systems for new applications, smaller
856 size scales, and at lower costs than what can be achieved
857 with current technology. As a result, time-variant ED
858 may have particular value as a potable water source for
859 poor, off-grid communities in developing countries.

Acknowledgements

This work was supported by the US Bureau of Recla-
mation DWPR program (R17AC00150, R18AC00109),
Tata Projects Ltd., Xylem Water Solutions and Water
Technology, and the MIT Energy Initiative. We would
like to thank Randall Shaw, Dan Lucero, and Fran-
cisco Nisino at BGNDRF for their technical support.
We would like to thank Elizabeth Brownell, Natasha
C. Wright, Rashed Al-Rashed, Sahil R. Shah, and San-
dra L. Walter for building the pilot system presented in
this work at BGNDRF, and for their fruitful discussions
about this research. I.M.P. and T.B. acknowledge the
support from Singapore's National Research Foundation
through the Singapore-MIT Alliance for Research and
Technology's 'Low energy electronic systems (LEES)
IRG'. W.H. acknowledges the support from the Royal
Academy of Engineering Research Fellowship to com-
plete this manuscript.

8. Reference

- [1] M. M. Mekonnen, A. Y. Hoekstra, Four billion people facing severe water scarcity, *Science advances* 2 (2) (2016) e1500323.
- [2] W. B. Group, High and dry: Climate change, water, and the economy, World Bank, 2016.
- [3] J. S. Stanton, D. W. Anning, C. J. Brown, R. B. Moore, V. L. McGuire, S. L. Qi, A. C. Harris, K. F. Dennehy, P. B. McMahon, J. R. Degnan, et al., Brackish groundwater in the united states, Tech. rep., US Geological Survey (2017).
- [4] SAO India, ground water quality in shallow aquifer of India, Available at <https://www.indiastat.com/table/villages/6376/ruralfacilities/281388/281420/data.aspx> (2018/08/23).
- [5] Groundwater in china: Part 1 - occurrence and use, Available at https://ecoinnovation.dk/media/mst/94641/130618%20Groundwater%20in%20China_Part%201_Occurrence%20and%20Use.pdf (2019/08/23).
- [6] B. D. Negewo, Renewable energy desalination: an emerging solution to close the water gap in the Middle East and North Africa, World Bank Publications, 2012.
- [7] N. Ghaffour, J. Bundschuh, H. Mahmoudi, M. F. Goosen, Renewable energy-driven desalination technologies: A comprehensive review on challenges and potential applications of integrated systems, *Desalination* 356 (2015) 94–114.
- [8] N. C. Wright, et al., Justification for community-scale photovoltaic-powered electrodialysis desalination systems for inland rural villages in india, *Desalination* 352 (2014) 82–91.
- [9] A. Campione, L. Gurreri, M. Ciofalo, G. Micale, A. Tamburini, A. Cipollina, Electrodialysis for water desalination: A critical assessment of recent developments on process fundamentals, models and applications, *Desalination* 434 (2018) 121–160.
- [10] M. Shatat, M. Worall, S. Riffat, Opportunities for solar water desalination worldwide, *Sustainable cities and society* 9 (2013) 67–80.
- [11] M. S. Miranda, D. Infield, A wind-powered seawater reverse-osmosis system without batteries, *Desalination* 153 (1-3) (2003) 9–16.
- [12] W. He, S. Amrose, N. C. Wright, T. Buonassisi, I. M. Peters, A. G. Winter, Field demonstration of a cost-optimized solar powered

917 electro dialysis reversal desalination system, Desalination, sub- 982
918 mitted. 983

919 [13] D. W. Bian, S. M. Watson, N. C. Wright, S. R. Shah, T. Buonas- 984
920 sasi, D. Ramanujan, I. M. Peters, et al., Optimization and design 985
921 of a low-cost, village-scale, photovoltaic-powered, electro dialy- 986
922 sis reversal desalination system for rural india, Desalination 452 987
923 (2019) 265–278. 988

924 [14] M. S. Ziegler, J. M. Mueller, G. D. Pereira, J. Song, M. Ferrara, 989
925 Y.-M. Chiang, J. E. Trancik, Storage requirements and costs of 990
926 shaping renewable energy toward grid decarbonization, Joule 991
927 3 (9) (2019) 2134–2153. 992

928 [15] H. Safaei, D. W. Keith, How much bulk energy storage is needed 993
929 to decarbonize electricity?, Energy & Environmental Science 994
930 8 (12) (2015) 3409–3417. 995

931 [16] Y. Wang, L. Li, Time-of-use electricity pricing for industrial 996
932 customers: A survey of us utilities, Applied Energy 149 (2015) 997
933 89–103. 998

934 [17] B. S. Richards, G. L. Park, T. Pietzsch, A. I. Schäfer, Renewable 999
935 energy powered membrane technology: Safe operating window 1000
936 of a brackish water desalination system, Journal of membrane 1001
937 science 468 (2014) 400–409. 1002

938 [18] G. L. Park, A. I. Schäfer, B. S. Richards, Renewable energy pow- 1003
939 ered membrane technology: The effect of wind speed fluctua- 1004
940 tions on the performance of a wind-powered membrane system 1005
941 for brackish water desalination, Journal of Membrane Science 1006
942 370 (1-2) (2011) 34–44.

943 [19] B. S. Richards, D. P. Capão, W. G. Früh, A. I. Schäfer, Re- 1007
944 newable energy powered membrane technology: Impact of solar 1008
945 irradiance fluctuations on performance of a brackish water re- 1009
946 verse osmosis system, Separation and Purification Technology 1000
947 156 (2015) 379–390.

948 [20] J. Shen, A. Jeyhanipour, B. S. Richards, A. I. Schäfer, Re- 1001
949 newable energy powered membrane technology: experimental 1002
950 investigation of system performance with variable module size 1003
951 and fluctuating energy, Separation and Purification Technology. 1004

952 [21] F. Cirez, J. Uche, A. Bayod, A. Martinez, Batch ed fed by a pv 1005
953 unit: a reliable, flexible, and sustainable integration, Desalina- 1006
954 tion and Water Treatment 51 (4-6) (2013) 673–685.

955 [22] P. Malek, Clean water from clean energy: removal of dissolved 1007
956 contaminants from brackish groundwater using wind energy 1008
957 powered electro dialysis, Ph.D. thesis, The University of Edin- 1009
958 burgh (2015).

959 [23] J. M. Veza, B. Peñate, F. Castellano, Electro dialysis desalination 1000
960 designed for wind energy (on-grid tests), Desalination 141 (1) 1001
961 (2001) 53–61.

962 [24] J. Veza, B. Peñate, F. Castellano, Electro dialysis desalination 1002
963 designed for off-grid wind energy, Desalination 160 (3) (2004) 1003
964 211–221.

965 [25] S. R. Shah, S. L. Walter, et al., Using feed-forward voltage- 1004
966 control to increase the ion removal rate during batch electro- 1005
967 dialysis desalination of brackish water, Desalination 457 (2019) 1006
968 62–74.

969 [26] S. R. Shah, N. C. Wright, P. A. Nepsky, A. G. Winter, Cost- 1007
970 optimal design of a batch electro dialysis system for domestic 1008
971 desalination of brackish groundwater, Desalination 443 (2018) 1009
972 198–211.

973 [27] N. C. Wright, S. R. Shah, S. E. Amrose, A. G. Winter, A rob- 1000
974 ust model of brackish water electro dialysis desalination with 1001
975 experimental comparison at different size scales, Desalination 1002
976 443 (2018) 27–43.

977 [28] M. Šavar, H. Kozmar, I. Sutlović, Improving centrifugal pump 1003
978 efficiency by impeller trimming, Desalination 249 (2) (2009) 1004
979 654–659.

980 [29] Y. Zhang, L. Pinoy, B. Meesschaert, B. Van der Bruggen, A 1005
981 natural driven membrane process for brackish and wastewater 1006
982 treatment: photovoltaic powered ed and fo hybrid system, Envi- 983
984 ronmental science & technology 47 (18) (2013) 10548–10555. 984
985 [30] R. P. Allison, Electro dialysis reversal in water reuse applica- 986
987 tions, Desalination 103 (1-2) (1995) 11–18. 987
988 [31] H. Strathmann, Electro dialysis, a mature technology with a mul- 988
989 titude of new applications, Desalination 264 (3) (2010) 268–288. 989
990 [32] M. H. Albadi, E. F. El-Saadany, A summary of demand response 990
991 in electricity markets, Electric power systems research 78 (11) 991
992 (2008) 1989–1996. 992
993 [33] Tata power launches TP renewable microgrid supported by 993
994 the Rockefeller Foundation, [https://www.tatapower.com/](https://www.tatapower.com/products-and-services/micro-grids.aspx) 994
995 [products-and-services/micro-grids.aspx](https://www.tatapower.com/products-and-services/micro-grids.aspx). 995
996 [34] K. M. Chehayeb, D. M. Farhat, K. G. Nayar, et al., Optimal de- 996
997 sign and operation of electro dialysis for brackish-water desalina- 997
998 tion and for high-salinity brine concentration, Desalination 420 998
999 (2017) 167–182. 999
1000 [35] H.-J. Lee, F. Sarfert, H. Strathmann, S.-H. Moon, Designing of 1000
1001 an electro dialysis desalination plant, Desalination 142 (3) (2002) 1001
1002 267–286. 1002
1003 [36] Y. Tanaka, A computer simulation of batch ion exchange mem- 1003
1004 brane electro dialysis for desalination of saline water, Desalina- 1004
1005 tion 249 (3) (2009) 1039–1047. 1005
1006 [37] Y. Kim, W. S. Walker, D. F. Lawler, Electro dialysis with spacers: 1006
1007 effects of variation and correlation of boundary layer thickness, 1007
1008 Desalination 274 (1-3) (2011) 54–63. 1008

9. Appendix

9.1. Appendix A: hydraulic diameter and the Sherwood number

In the mass transfer coefficient k , the hydraulic diameter d_h is

$$d_h = \frac{4\epsilon}{2/h + (1 - \epsilon)(8/h)}, \quad (19)$$

where ϵ is the void fraction. The Sherwood Number, a measure of mass transfer performance, is correlated to the Reynolds Number and the Schmidt number by

$$Sh = aRe^b Sc^c. \quad (20)$$

The Schmidt number Sc is a material dependent, non-dimensional quantity relating the momentum and mass diffusion. The Reynolds number is a dimensionless number relating inertial to viscous stresses in the flow. They are

$$Sc = \frac{\mu}{\rho_{aq} D_{aq}} \quad (21)$$

and

$$Re = \frac{\rho_{aq} u_{ch} d_h}{\mu}. \quad (22)$$

9.2. Appendix B: The pump curve used in this paper

Two pumps were used in the ED system presented: a diluate pump and a concentrate pump. The two pumps were the same model, but the performance slightly varied

1019 due to differences in their associated hydraulic circuits
 1020 in the ED system. In order to mitigate the fouling, elec-
 1021 trodialysis reversal (EDR) operation was used during
 1022 testing, such that the polarity of the electrical field was
 1023 reversed after each batch. As a result, each pump operated
 1024 in two positions, namely position 1 and position 2.
 1025 Figure 10 presents the experimentally measured pump
 1026 curves, which were used to predict pump performance
 1027 in this work.

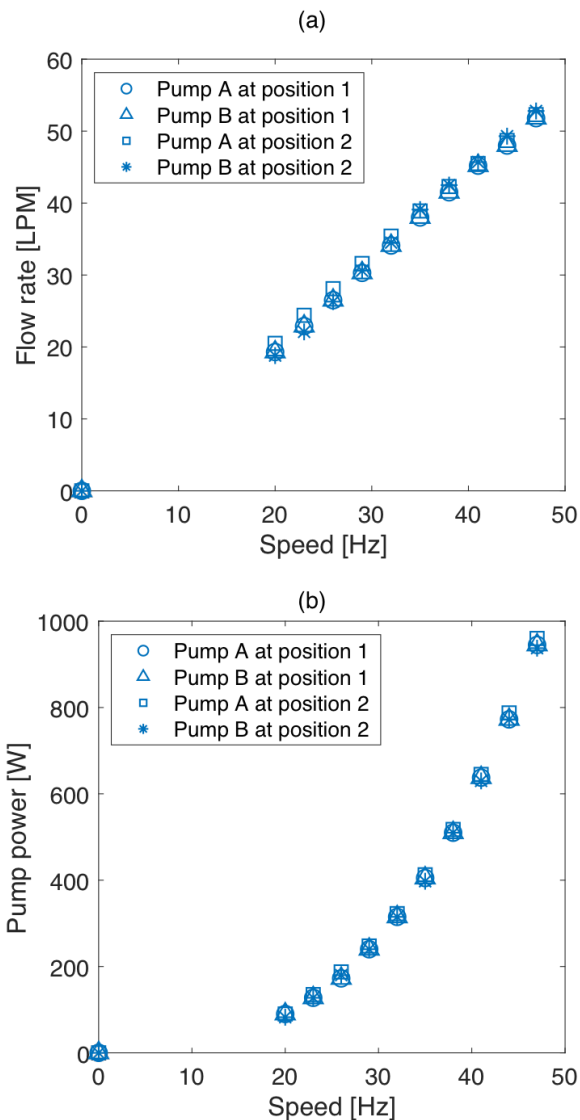


Figure 10: Pumps curves of the two pumps used in the pilot time-variant ED system.

9.3. Appendix C: Desalination rate of CVCQ at different flow rates

An appropriate flow velocity is determined by the trade-off between pumping power and ED stack power consumption, which is expected to be small enough to reduce pumping power, but just high enough to increase the limiting current density and to limit concentration polarization [34]. Consequently, the flow rate of a conventional ED batch is usually between 4–10 cm/s in each membrane channel according to prior experimental and theoretical studies [35, 36, 37], and the manufacture’s recommended flow rate of (~7 cm/s) [27]. Therefore, Fig. 11 presents the desalination performance of static ED operation with several flow rates for potential comparisons.

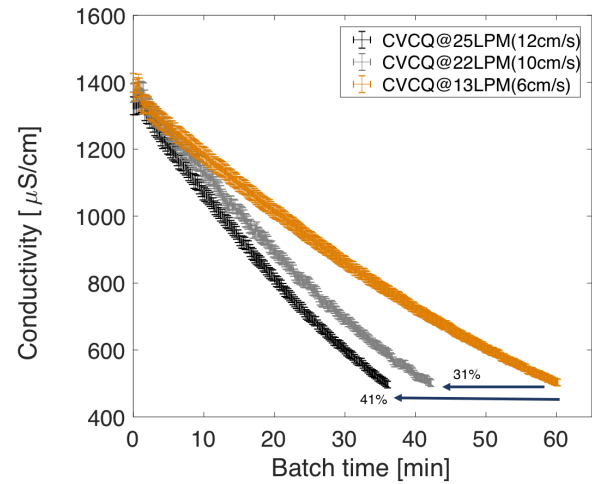


Figure 11: The diluate conductivity versus the batch time of CVCQ operation at various flow rates.

Acronyms

- AEM Anion exchange membranes.
- BGNDRF Brackish Groundwater National Desalination Research Facility.
- CapEx Captial expenditure.
- CEM cation exchange membranes.
- CVCQ Constant voltage constant flow rate.
- DC Direct current.
- DR Demand response.

1053	ED Electro dialysis.	V_{el} Electrode potential, V	1088
1054	OpEx Operational expenditure.	V Voltage, V	1089
1055	PLC Programmable logic controller.	V^{cell} Volume of a cell, m^3	1090
1056	PV Photovoltaic.	V^{tank} Volume of tank, m^3	1091
1057	RO Reverse osmosis.	W Stack width, m	1092
1058	SEC Specific energy consumption.	z Ion charge	1093
1059	TDS Total dissolved solids.	ϕ_A Open-area porosity of the spacer	1094
1060	VFD Variable frequency drive.	ϕ Current leakage factor	1095
1061	VVCQ Variable voltage constant flow rate.	τ Control time, s	1096
1062	VVVQ Variable voltage variable flow rate.	Superscript and subscript	1097
1063	Symbols	0 Position in the tank	1098
1064	A Membrane area, m^2	AEM Anion exchange membrane	1099
1065	C_c^b Bulk concentration of concentrate, $mol\ m^{-3}$	CEM Cation exchange membrane	1100
1066	C_d^b Bulk concentration of diluate, $mol\ m^{-3}$	y Position at the segment y	1101
1067	d_h Hydraulic diameter, m	Y Position at the segment Y	1102
1068	D Diffusion coefficient, $m^2\ s^{-1}$	τ_i Control time step i	1103
1069	F Faraday constant, $96485\ C\ mol^{-1}$		
1070	H Pump head, m		
1071	i Current density, $A\ m^{-2}$		
1072	I Current, A		
1073	k Mass transfer coefficient, $m\ s^{-1}$		
1074	L Membrane channel length, m		
1075	N Number of cell pairs		
1076	P Power, W		
1077	Q_c Flow rate of concentrate, $m^3\ s^{-1}$		
1078	Q_d Flow rate of diluate, $m^3\ s^{-1}$		
1079	r_i Safety factor		
1080	R Resistance, Ω		
1081	Sh Sherwood Number		
1082	t Time, s		
1083	T Temperature, K		
1084	$t^{AEM,CEM}$ Transport numbers of the AEM and CEM		
1085	membranes		
1086	$t^{+,-}$ Minimum of the anion and cation transport num-		
1087	bers		